Available online at www.sciencedirect.com
ScienceDirect
Electric Power Systems Research 77 (2007) 447–454
ELECTRIC POWER SYSTEMS RESEARCH
www.elsevier.com/locate/epsr

Indirect matrix converter drives for unity displacement factor and minimum switching losses

Sangshin Kwak *

Research & Development Center, Samsung SDI Co. Ltd., Youngin, Republic of Korea

Received 2 January 2006; received in revised form 17 April 2006; accepted 22 April 2006
Available online 21 June 2006

Abstract

With sinusoidal input currents and no dc-link capacitor, a matrix converter offers remarkable advantages over other alternatives in applications requiring improved utility interaction and critical weight/volume reduction. Lately, indirect matrix converter topologies have also been investigated, leading to possibility of reduced switch number and multi-drive applications. However, due to off-line input current regulation of the converters, the input displacement factor varies with LC input filters and load conditions. This fact results in non-unity displacement factor and increased reactive power flow. In this paper, a novel on-line input current control strategy is proposed based on a closed-loop control in the synchronous reference frame. The approach allows independent control of two input current components (active and reactive), yielding zero reactive components. In addition, this paper specifies a relationship of input current phase angle and switching losses in semiconductors. Based on the specification, it is proved that the indirect matrix converter has minimum switching losses with the input currents in phase with the input voltages. Thus, the proposed control algorithm yields minimum switching losses and no reactive power flow. The feasibility of the proposed technique has been verified in the paper.

Keywords: Matrix converter; On-line input current control; Unity power factor

1. Introduction

Advances in power semiconductor technology and low-cost control processes have significantly matured the adjustable speed drives (ASDs) with concomitant reductions of energy consumption in industrial processes. The research efforts of the ASD technologies have been mostly dominated by investigation of inverter-motor assembly to achieve better output performance characteristics. As the output performances of the ASDs have continued to improve, the research trends for the ASDs, in recent years, have been focused on improved interaction with the utility to provide clean power distribution system. Realizing more compact and efficient ASDs has also been an important issue. The matrix converter has recently received considerable interests, because it possesses the topological and operational features to fulfill these current trends for the ASDs [1,2]. The matrix converter can reduce its converter size by eliminating bulky dc-link components and becomes a better candidate in ASD applications with reduced weight and volume requirements. In addition, the matrix converter causes no harmonic problems in the utility supply with its ability to generate sinusoidal input currents.

A traditional matrix converter configuration is based on a direct ac/ac power conversion by directly connecting three-phase input voltages to three-phase output loads through bi-direction switches with no intermediate power conversion stage [1–3]. Alternative topologies have lately been investigated to implement the matrix converters, based on ac/dc/ac power conversion with no dc-link capacitor [4–7]. The matrix converter topology, called the indirect matrix converter, has shown several advantages over the traditional direct matrix converter. Because it has converter configuration with two separate stages (rectifier and inverter stages), it has been considered more flexible to modify its topology. This feature resulted in topological modifications with reduced switch numbers and its extension to multi-drive applications [7,8]. In conventional control strategies for the indirect matrix converter, the rectifier stage has been operated with off-line pulsewidth modulation (PWM) switching patterns [4]. The PWM scheme depends only on the supply voltage angle.

* Tel.: +82 31 288 4793; fax: +82 31 288 4777.
E-mail address: sskwak@ieee.org.

0378-7796/$ – see front matter © 2006 Elsevier B.V. All rights reserved.
doi:10.1016/j.epsr.2006.04.012

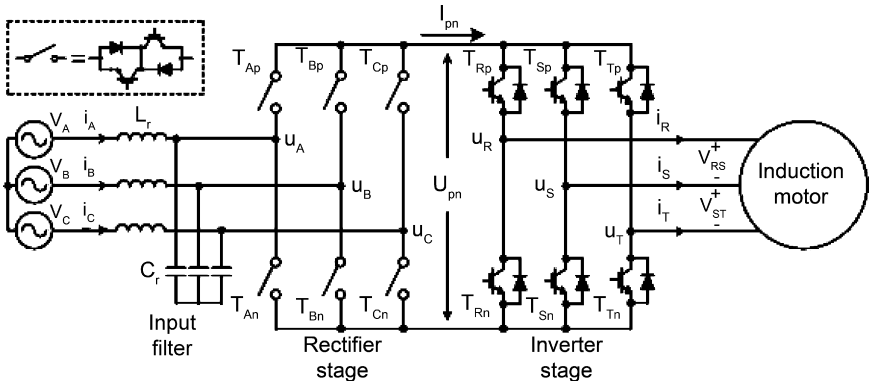

Fig. 1. Indirect matrix converter topology.

As a result, the input currents in the converter, despite of sinusoidal waveforms, have either leading or lagging power factor, according to input LC filters and load conditions. This fact yields the non-unity displacement factor and the reactive power flow through the matrix converter.

In this paper, the conventional control scheme for the rectifier stage in the indirect matrix converter is reviewed and its space vector diagram is derived. Based on the derived vector diagram, this paper proposes a novel on-line control approach to the input currents. The approach utilizes the input current feedback technique and its on-line regulation in the synchronous reference frame. In addition, this paper specifies a relationship between the switching losses in the indirect matrix converter and the input displacement factor, and shows that the indirect matrix converter has minimum losses in case of unity displacement factor. Thus, the proposed closed-loop input current regulation method in the synchronous reference frame ensures the unity displacement factor in the matrix converter and the minimum switching losses. Following improved features are obtained: (1) independent control of active and reactive power components in the input currents; (2) guaranteed unity power factor due to the unity displacement factor, regardless of input filters and load conditions; (3) minimum switching losses; (4) no reactive power flow through the indirect matrix converter; and (5) complete closed-loop control for both input and output currents.

2. Indirect matrix converter

A circuit topology of the indirect matrix converter is illustrated in Fig. 1. The basic concept of the indirect matrix converter is to separate the ac/ac conversion into two stages, such as the rectifier and the inverter stages with no dc-link capacitor [4,8]. The rectifier stage is composed of six bi-directional switches built with 12 unidirectional switches, while the inverter stage has six unidirectional switches. As a result, independent switching modulation strategies can be used for each stage. The purpose of the rectifier is generating the sinusoidal input currents as well as maintaining a constant local-averaged dc output voltage in the dc-link, by modulating the two line-to-line input voltages. Output voltages with variable frequency and variable amplitude can be obtained through the conventional space vector PWM modulation of the inverter stage, using the constant dc voltage obtained from the rectifier stage. The input LC filter is installed to filter out high frequency PWM components of the input currents.

The modulation scheme for the rectifier stage is performed with the off-line PWM pattern, depending only on the phase angle of the supply voltage [4]. For example, consider the instant that the supply voltage v_A is positive, while v_B and v_C are negative. In this condition, the upper switch in A-phase, T_{Ap} stays on. On the other hand, T_{Bn} and T_{Cn} are modulated to achieve the constant and maximum dc voltage in the dc-link and sinusoidal input currents. Therefore, the switch T_{Ap} performs no switching action in this period. The modulation functions for the switches, T_{Bn} and T_{Cn}, are only dependent on the phase angle of the supply voltage. Likewise, the switching status and the modulation functions of the six switches in the rectifier stage are determined by the supply voltage angle. Fig. 2 summarizes the sectors and the switch status in the rectifier stage, according to the supply voltage angle. S_{on} denotes a switch in the on state, and S_{mod} is a modulating switch in one sector, respectively. A space vector diagram is derived from the switching conditions shown in Fig. 2. Assume three-phase balanced supply voltages given by

$$v_A(\omega t) = V_m \cos(\omega t), \qquad v_B(\omega t) = V_m \cos\left(\omega t - \frac{2\pi}{3}\right),$$
$$v_C(\omega t) = V_m \cos\left(\omega t + \frac{2\pi}{3}\right) \tag{1}$$

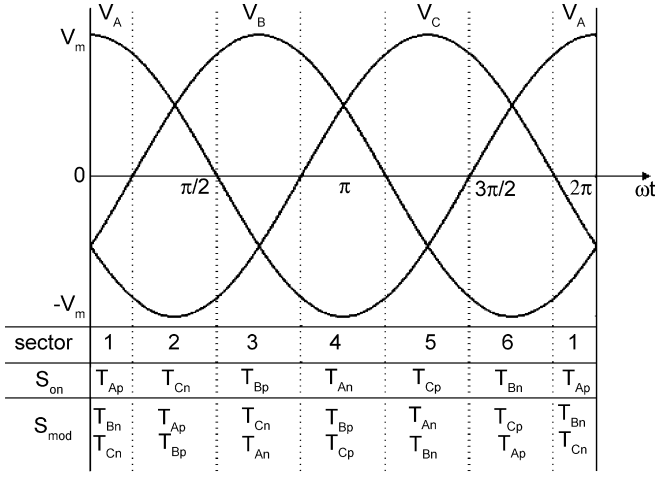

Fig. 2. Switch conditions of rectifier stage based on input voltages.

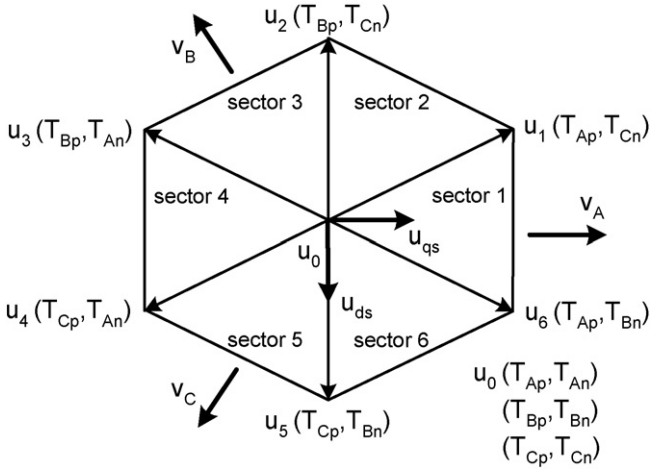

Fig. 3. Space vector diagram of rectifier stage.

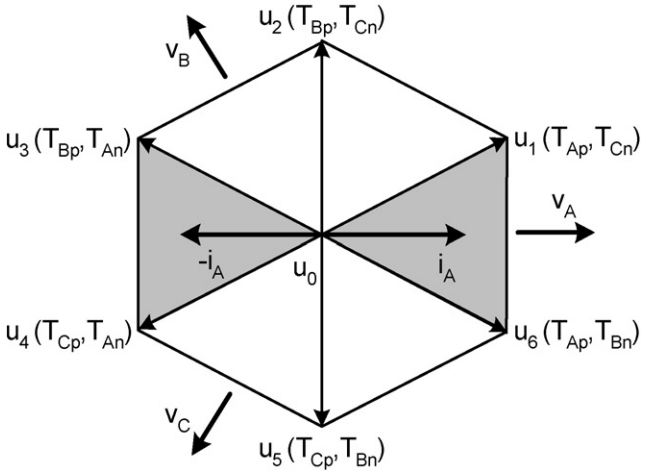

Fig. 4. Switching diagram of rectifier stage operating with unity displacement factor.

where, V_m and ω denote the amplitude and the angular frequency of the supply voltage, respectively. For deriving and modeling the space vector diagram in the rectifier stage, the voltages of the rectifier stage, u_A, u_B, and u_C are transformed into the stationary reference frame as

$$\begin{bmatrix} u_{qs} \\ u_{ds} \end{bmatrix} = \frac{2}{3} \begin{bmatrix} 1 & -\frac{1}{2} & -\frac{1}{2} \\ 0 & -\frac{\sqrt{3}}{2} & \frac{\sqrt{3}}{2} \end{bmatrix} \begin{bmatrix} u_A \\ u_B \\ u_C \end{bmatrix} \quad (2)$$

Based on the switching status shown in Fig. 2 and (2), the space vector diagram can be obtained. It should be noticed that no freewheeling paths in the conventional PWM rectifier with unidirectional switches such as insulated gate bipolar transistor (IGBT) exist in the rectifier stage of the matrix converter, since the switch cells of the matrix converter are composed of controllable bi-directional switches. Thus, the corresponding rectifier voltage is equal to zero in case that both switches in one leg are turned off. Fig. 3 shows the space vector diagram derived in the rectifier stage.

From Figs. 2 and 3, it is seen that this PWM strategy distributes 120° intervals of a non-switching region to each rectifier leg, by alternatively connecting each rectifier leg to the positive or negative rail of the dc-link. In other words, every bi-directional switch cell occupies a 60° non-modulating segment in one supply voltage cycle. Thus, it can be concluded that the PWM scheme in the rectifier stage of the indirect matrix converter is based on the discontinuous switching operation, namely, the discontinuous PWM scheme. It is worth noting that the switching losses in the discontinuous PWM strategy depend on the location of non-modulating segments in the vector diagram [9]. The switching losses in the discontinuous PWM method can be minimized by distributing the 60° non-switching intervals to positive and negative peak input currents, respectively. This minimum switching loss condition occurs due to the absence of the switching operation in the regions of peak input currents, where the highest switching losses are caused. Thus, the displacement factor of the indirect matrix converter is directly related to the switching losses of the semiconductor in the entire system. Fig. 4 shows the switching diagram of the rectifier stage operating with the unity displacement factor, where the shaded areas illustrate non-modulating areas of the switches T_{Ap} and T_{An}. In Fig. 4, it is shown that the upper and lower switches in each phase are fixed to the ON or OFF state with no switching action in the peak input current region, only if the matrix converter operates with the unity displacement factor. This will lead to the minimum switching losses, in case that the input currents are in phase with the input voltages. Therefore, the minimum switching losses can be obtained under unity displacement factor condition. Otherwise, the switch cells of the rectifier stage will have a switching region in vicinity of the peak input current, yielding increased switching losses. Because the rectifier stage in the indirect matrix converter operates with 12 IGBTs at high switching frequency, the minimization of the switching losses in the rectifier stage is quite important.

In conventional PWM strategy explained above, the rectifier stage of the indirect matrix converter has been operated with the off-line PWM pattern, which depends only on the phase angle of the supply voltage. Accordingly, the control scheme exhibits a load-dependent displacement factor, with the presence of the LC input filter in the matrix converter topology. Thus, the minimum switching losses and reactive power suppression are not guaranteed with the conventional off-line PWM scheme in the matrix converter.

3. Proposed control scheme for indirect matrix converter

3.1. Rectifier stage

The on-line input current regulation for the indirect matrix converter is developed to obtain the unity displacement factor and the minimum switching losses, irrespective of the input filters and the load conditions. The proposed scheme independently controls the active and the reactive power components of the input currents. This control strategy is based on the feedback current control technique in the synchronous reference frame.

From Fig. 1, the rectifier on the ac side can be modeled as

$$u_A = v_A - L_r\left(\frac{di_A}{dt}\right), \qquad u_B = v_B - L_r\left(\frac{di_B}{dt}\right),$$
$$u_C = v_C - L_r\left(\frac{di_C}{dt}\right) \tag{3}$$

where, u_A, u_B, and u_C represent the ac terminal voltages of the rectifier, respectively. To design the control system of the rectifier stage in the synchronous frame, the voltages and currents of the rectifier stage in abc stationary reference frame are transformed to the synchronous frame as

$$\begin{bmatrix} V_{qr} \\ V_{dr} \end{bmatrix} = \frac{2}{3}\begin{bmatrix} \cos\theta & \cos\left(\theta - \frac{2\pi}{3}\right) & \cos\left(\theta + \frac{2\pi}{3}\right) \\ \sin\theta & \sin\left(\theta - \frac{2\pi}{3}\right) & \sin\left(\theta + \frac{2\pi}{3}\right) \end{bmatrix}\begin{bmatrix} v_A \\ v_B \\ v_C \end{bmatrix} \tag{4}$$

$$\begin{bmatrix} I_{qr} \\ I_{dr} \end{bmatrix} = \frac{2}{3}\begin{bmatrix} \cos\theta & \cos\left(\theta - \frac{2\pi}{3}\right) & \cos\left(\theta + \frac{2\pi}{3}\right) \\ \sin\theta & \sin\left(\theta - \frac{2\pi}{3}\right) & \sin\left(\theta + \frac{2\pi}{3}\right) \end{bmatrix}\begin{bmatrix} i_A \\ i_B \\ i_C \end{bmatrix} \tag{5}$$

where, the subscript 'r' denotes the 'q' and 'd' components of currents and voltages in the rectifier stage, and θ is the phase angle of the input supply ($\theta = \omega t$).

The rectifier model on the ac side in (3) can be now written in the synchronous reference frame by

$$\begin{bmatrix} U_{qr} \\ U_{dr} \end{bmatrix} = \begin{bmatrix} -L_r\left(\frac{d}{dt}\right) & -\omega L_r \\ \omega L_r & -L_r\left(\frac{d}{dt}\right) \end{bmatrix}\begin{bmatrix} I_{qr} \\ I_{dr} \end{bmatrix} + \begin{bmatrix} V_{qr} \\ V_{dr} \end{bmatrix} \tag{6}$$

Assuming that the matrix converter is fed from a three-phase balanced voltage set, the supply voltages in the synchronous frame, V_{qr} and V_{dr}, are decoupled using (1) and (4) as

$$V_{qr} = V_m, \qquad V_{dr} = 0 \tag{7}$$

The complete rectifier model on its ac side in the synchronous frame is

$$\begin{bmatrix} U_{qr} \\ U_{dr} \end{bmatrix} = \begin{bmatrix} -L_r\left(\frac{d}{dt}\right) & -\omega L_r \\ \omega L_r & -L_r\left(\frac{d}{dt}\right) \end{bmatrix}\begin{bmatrix} I_{qr} \\ I_{dr} \end{bmatrix} + \begin{bmatrix} V_m \\ 0 \end{bmatrix} \tag{8}$$

The active and reactive power requirements of the rectifier stage, P_r^* and Q_r^*, are expressed as

$$P_r^* = \left(\frac{3}{2}\right)(V_{qr}I_{qr}^* + V_{dr}I_{dr}^*), \qquad Q_r^* = \left(\frac{3}{2}\right)(V_{dr}I_{qr}^* - V_{qr}I_{dr}^*) \tag{9}$$

For unity power factor operation, the reactive power of the rectifier stage is set to zero. From $Q_r^* = 0$, (7) and (9), the input current requirements are written by

$$\begin{bmatrix} I_{qr}^* \\ I_{dr}^* \end{bmatrix} = \begin{bmatrix} \frac{2P_r^*}{3V_m} \\ 0 \end{bmatrix} \tag{10}$$

The current requirement of the d-axis components I_{dr}^* is regulated to zero for unity displacement factor, including the effect of the input filters on the current phase shift. On the other hand, the q-axis component I_{qr}^* depends on the active power of the rectifier stage, which is ideally equal to the output power of the inverter stage. This implies that knowledge of the output power for the inverter stage should be feedforwarded to the rectifier stage, in order to determine the q-axis current command.

The desired rectifier vector U_{rec} is composed of two orthogonal elements as

$$U_{rec} = U_{qr} + jU_{dr} \tag{11}$$

It is obvious that the desired vector components U_{qr} and U_{dr} can be generated by the two adjacent active vectors of each sector and the zero vector as shown in Fig. 3, depending on the input voltage phase angle. For instance, if the desired vector is in the sector 1, it is synthesized by modulating T_{Cn} and T_{Bn}, while T_{Ap} keeps on. The on-times of the modulating switches T_{Bn} and T_{Cn} are dependent on the angle θ_{rec}, as shown in Fig. 5. The duty cycles of the switches are obtained with the laws of sines as

$$d_{\alpha r} = d_{TBn} = m_c \sin(60^\circ - \theta_{rec}), \qquad d_{\beta r} = d_{TCn} = m_c \sin(\theta_{rec}) \tag{12}$$

where, $m_c = I_{im}/I_{pn}$. I_{im} and I_{pn} denote the peak values of the input currents and the dc-link current magnitude, respectively. In the rectifier stage, the modulation index m_c is set to unity to achieve maximum attainable voltage in the dc-link. Note that the zero vectors are inherently generated by the controller. However, the zero vectors in the rectifier stage will reduce the local-averaged dc-link voltage, by making the dc-link voltage zero. Moreover, the zero vectors lead to abrupt voltage fluctuation from line-to-line voltage to zero in the dc-link, which may cause potential hazard in the semiconductor breakdown. Fig. 6 illustrates the input currents and the dc-link voltage with zero

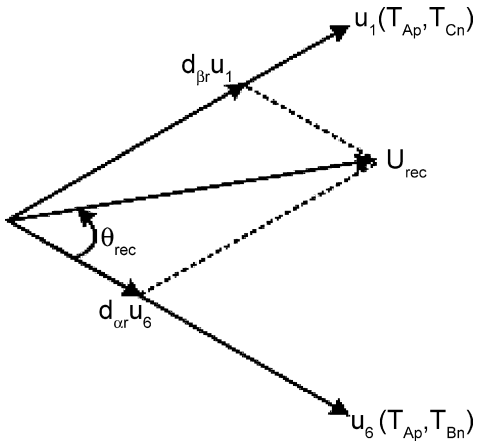

Fig. 5. Vector composition in rectifier stage.

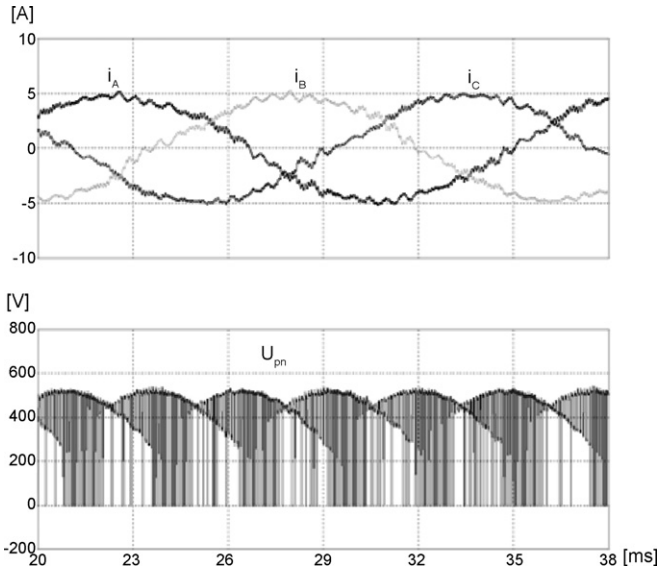

Fig. 6. Input currents and dc-link voltage with zero vectors.

vectors. It is seen that the voltage U_{pn} becomes zero when the controller assumes the zero vectors. Thus, a normalizing factor is introduced for eliminating the zero voltage vectors produced by the controller. In case that the rectifier sector 1 is activated, a normalizing factor N is derived so that the operation of the modulating switches occupy the entire switching periods as

$$\frac{1}{N}(d_{TBn} + d_{TCn}) = 1 \tag{13}$$

The angle in the sector 1 is

$$\theta_{rec} = \omega t + 30^\circ, \quad -30^\circ \le \omega t \le 30^\circ \tag{14}$$

Substituting (12) and (14) into (13) yields the normalizing factor N for the sector 1 as

$$N = \cos \omega t, \quad -30^\circ \le \omega t \le 30^\circ \tag{15}$$

The normalizing factors are, using the same approaches, determined for all the rectifier sectors. Table 1 shows the normalizing factor according to the sectors. By applying the normalizing factors, the desired rectifier voltage vectors are generated with only the active vectors. Furthermore, introducing the normalizing factor ensures that only one commutation between

Table 1
Normalizing factor of rectifier stage

Sector	Normalizing factor (N)
1	$\cos(\omega t)$
2	$-\cos\left(\omega t + \frac{2\pi}{3}\right)$
3	$\cos\left(\omega t - \frac{2\pi}{3}\right)$
4	$-\cos(\omega t)$
5	$\cos\left(\omega t + \frac{2\pi}{3}\right)$
6	$-\cos\left(\omega t - \frac{2\pi}{3}\right)$

the modulating switches occurs per the switching period T_s. The minimum number of the switching operation leads to the minimum switching losses, in conjunction with the unity displacement power factor. Note that the normalizing factor does not produce any singular points in the rectifier controller. The current control block diagram for the rectifier stage in the synchronous reference frame is shown in Fig. 7. In the entire control block, final switching signals are free from the zero vectors by the normalizing factor block N, which can be implemented with a look-up table storing the samples of the sinusoidal values.

3.2. Inverter stage

Because the constant local-averaged dc-link voltage is achieved in the rectifier stage, common space vector control algorithm can be applied for the inverter stage. The synchronous reference frame controller for the inverter stage is shown in Fig. 8. As similar with the voltage model in the rectifier stage, the output voltage model of the inverter in the synchronous reference frame is given by

$$\begin{bmatrix} U_{qi} \\ U_{di} \end{bmatrix} = \begin{bmatrix} \sigma L_s \left(\frac{d}{dt}\right) & \omega_e \sigma L_s \\ -\omega_e \sigma L_s & \sigma L_s \left(\frac{d}{dt}\right) \end{bmatrix} \begin{bmatrix} I_{qi} \\ I_{di} \end{bmatrix} + \begin{bmatrix} V_{qi} \\ V_{di} \end{bmatrix} \tag{16}$$

where, the subscript 'i' denotes the 'q' and 'd' components in the inverter currents. L_s, σ, and ω_e are the inductance, the total leakage factor, and the angular frequency of a load induction motor, respectively. In addition, V_{di} and V_{qi} imply the back-EMF of the induction motor. The rotor flux is oriented to the d-axis and controlled to a constant level in case of an indirect rotor-flux orientation strategy [10]. Thus, the back-EMF terms can be added

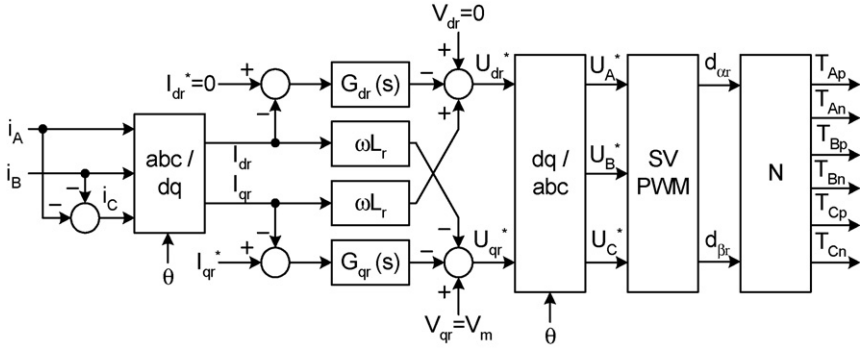

Fig. 7. Control block diagram of rectifier stage.

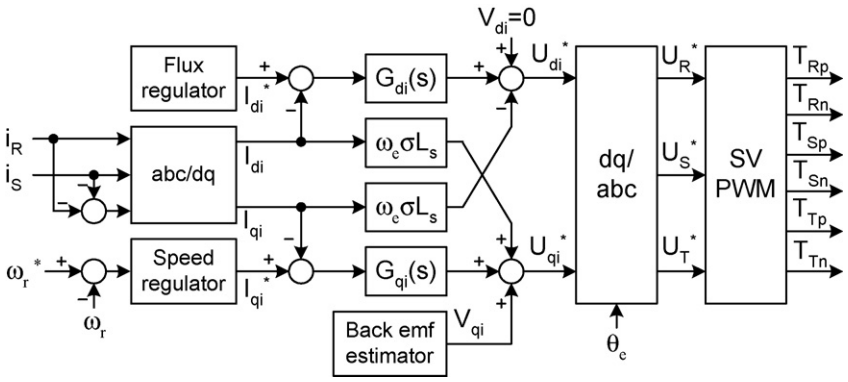

Fig. 8. Control block diagram of inverter stage.

in the inverter stage controller as the feedforward compensation components, in order to speed up current responses as shown in Fig. 8 [10]. The q-axis back-EMF is obtained by the back-EMF estimator block.

The q-axis current command in the rectifier stage is set based on the output power command delivered by the inverter [11]. As consequence, the output power requirement of the induction motor should be calculated and feedforwarded to the rectifier stage fast and accurately. The required output power, P^*_{out}, is directly estimated from the output voltage and current commands in the synchronous reference frame as

$$P^*_{\text{out}} = \frac{3}{2}(V^*_{\text{di}} I^*_{\text{di}} + V^*_{\text{qi}} I^*_{\text{qi}}) \tag{17}$$

However, determining the input current command from the output power requirement alone is not enough to maintain the power command of the induction motor, due to the power converter losses. Therefore, the minor feedback control loop is required to execute the function of the loss compensation. This function is normally performed by the dc-link capacitor voltage regulator in the back-to-back inverter systems with the dc-link capacitor [10,11]. On the other hand, since the indirect matrix converter has no dc-link capacitor, a direct output power controller is proposed to compensate the converter losses. The actual output power, P_{out}, is calculated based on the sensed output voltage and current of the induction motor and fed back to an output power regulator with the output power command, P^*_{out}. The active input current component of the rectifier stage, I^*_{qr} is

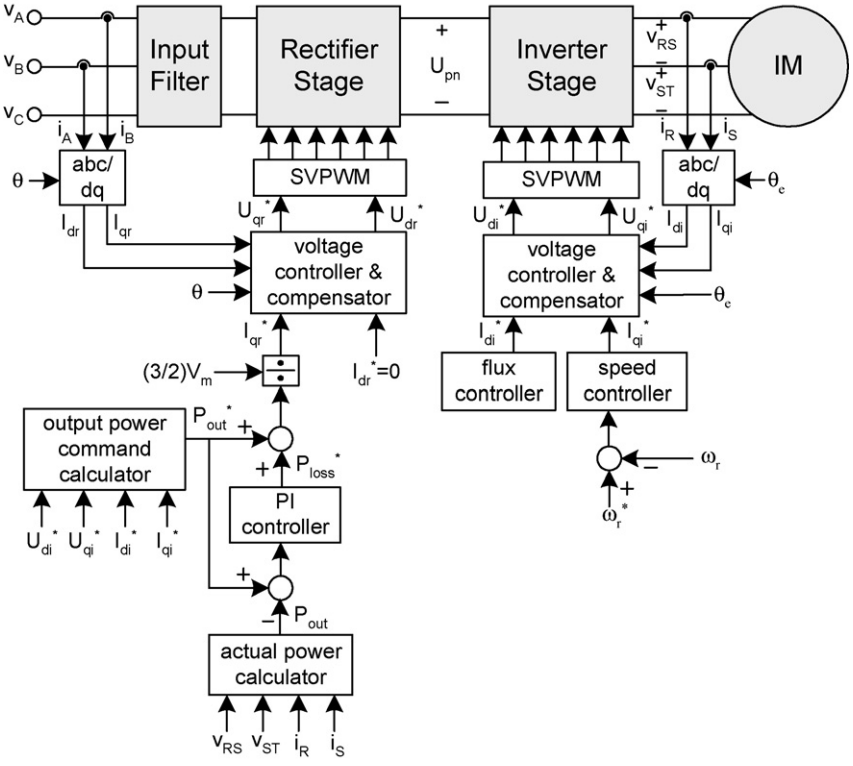

Fig. 9. Overall control block diagram of proposed matrix converter system.

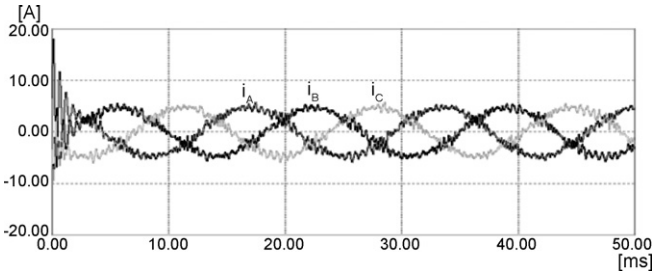

Fig. 10. Three-phase input currents of matrix converter.

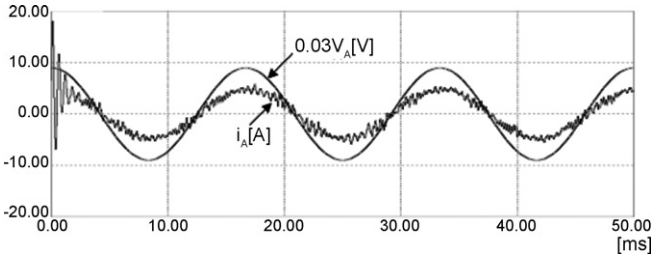

Fig. 11. Input phase voltage and current of matrix converter.

decided from both output power estimation and loss compensation terms. Fig. 9 shows the overall control block diagram of the proposed indirect matrix converter control algorithm based on the synchronous reference frame.

4. Verification results

A simulation was performed to verify the feasibility of the proposed control structure for the indirect matrix converter. The system simulation was made utilizing PSIM simulator incorporated with C compiler. Fig. 10 shows the three-phase input currents of the matrix converter controlled by the proposed on-line control scheme. It can be seen that the input current waveforms are essentially sinusoidal. This result demonstrates that the proposed control strategy produces no low-order harmonics in the input currents. Fig. 11 shows the input phase voltage and current of the matrix converter. It is seen that the input current is in phase with the input voltage, resulting in the unity displacement factor and minimum losses regardless of the input filter and the load. This feature is obtained by the closed-loop input current control. Fig. 12 shows the three-phase output currents of the matrix converter to feed the induction motor. It is seen

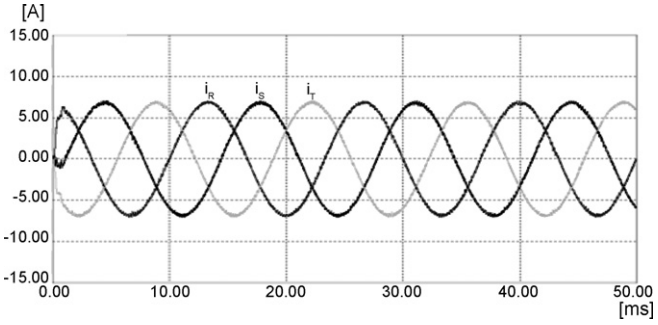

Fig. 12. Three-phase output voltages of matrix converter.

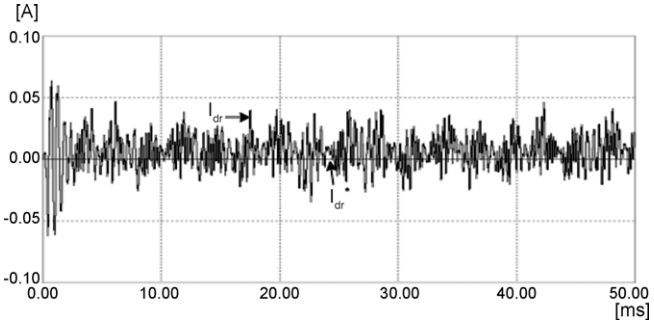

Fig. 13. *d*-Axis reference and actual currents in rectifier stage.

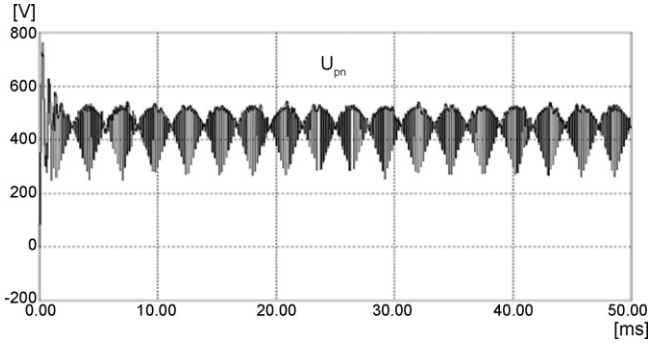

Fig. 14. dc-link voltage of matrix converter.

that the sinusoidal output currents with variable frequency and variable amplitude are generated to implement the vector control scheme of the induction motor. As seen in Figs. 10 and 12, the input currents show bigger current ripples than the output currents. This is due to the fact that the rectifier stage operates with the two-phase modulation, where only two rectifier phases commutates within the sampling period T_s. Meanwhile, three phases in the inverter stage are involved for switching operation during the same period T_s, leading reduced ripple magnitude compared to the two-phase switching operation. Fig. 13 shows the *d*-axis reference and actual currents in the rectifier stage of the matrix converter. The command current of the *d*-axis is set to zero in order to obtain the zero reactive power components and the unity displacement factor. It is shown that the actual *d*-axis current is regulated to follow the reference current using the synchronous reference frame based controller. Fig. 14 shows the dc-link voltage of the indirect matrix converter. It can be seen that the dc-link voltage is modulated between the two line-to-line voltages in order to obtain the constant local-averaged voltage. It should be noticed that the voltage U_{pn} does not decrease to zero because the normalizing factor forces no zero vectors produced in the rectifier stage.

5. Conclusions

This paper presents a novel control strategy for the indirect matrix converter based on the synchronous reference frame. The on-line input current control for the rectifier stage of the indirect matrix converter is developed to obtain the unity displacement factor. This feature is achieved by controlling the input currents using the closed-loop control scheme. The pro-

posed control strategy allows the unity displacement factor and no reactive power flow for the indirect matrix converter, regardless of the input filter and load effect. Moreover, it distributes non-modulated segments for the bi-directional switches of the rectifier stage in vicinity of the input peak current, resulting in the minimum switching losses in the matrix converter.

References

[1] M. Venturini, A new sine wave in, sine wave out conversion technique eliminates reactive elements, in: Proceedings of the POWERCON 7, 1980, pp. E3-1–E3-15.
[2] L. Huber, D. Borojevic, Space vector modulated three-phase to three-phase matrix converter with input power factor correction, IEEE Trans. Ind. Appl. 31 (6) (1995) 1234–1246.
[3] P.W. Wheeler, J.C. Clare, L. Empringham, A vector controlled MCT matrix converter induction motor drive with minimized commutation times and enhanced waveform quality, in: Proceedings of the IEEE-IAS Annual Meeting, vol. 1, 2002, pp. 466–471.
[4] L. Wei, T.A. Lipo, A novel matrix converter topology with simple commutation, in: Proceedings of the IEEE-IAS Annual Meeting, vol. 3, 2001, pp. 1749–1754.
[5] S. Kwak, H.A. Toliyat, Development of modulation strategy for two-phase AC–AC matrix converter, IEEE Trans. Energy Conver. 20 (2) (Jun. 2004) 493–494.
[6] S. Kwak, Design and analysis of modern three-phase AC/AC power converters for ac drives and utility interfaces, Ph.D. dissertation, Texas A&M University, 2005.
[7] J.W. Kolar, M. Baumann, F. Schafmeister, H. Ertl, Novel three-phase AC–DC–AC sparse matrix converter, in: Proc. IEEE APEC'02, vol. 2, 2002, pp. 287–292.
[8] C. Klumpner, F. Baabjerg, A new cost-effective multi-drive solution based on a two-stage direct power electronic conversion topology, in: Proceedings of the IEEE-IAS Annual Meeting, vol. 1, 2002, pp. 444–452.
[9] D.W. Chung, S.K. Sul, Minimum-loss strategy for three-phase PWM rectifier, IEEE Trans. Ind. Electron. 46 (3) (1999) 517–526.
[10] J.C. Liao, S.N. Yeh, A novel instantaneous power control strategy and analytic model for integrated rectifier/inverter system, IEEE Trans. Power Electron. 15 (6) (2000) 996–1006.
[11] L. Malesani, L. Rossetto, P. Tenti, P. Tomasin, AC/DC/AC PWM converter with reduced energy storage in the DC link, IEEE Trans. Ind. Appl. 31 (2) (1995) 287–292.

Sangshin Kwak received the B.S. and M.S. degree in electronics engineering from Kyungpook National University, Daegu, Korea, in 1997 and 1999, respectively, and the Ph.D. degree in electrical engineering from Texas A&M University, College Station, TX in 2005. From 1999 to 2000, he was a Research Engineer at LG Electronics, Korea. He was also with the Whirlpool R&D Center, Benton Harbor, MI, in 2004. Since 2005, he has been a Senior Engineer with R&D Center, Samsung SDI Co., Korea. His main research interests are topology design, control, modeling, and analysis of ac/dc, dc/ac, ac/ac power converters including resonant converters, adjustable speed drives, DSP-embedded power electronics control, and digital display drivers for plasma display panels. Dr. Kwak was listed in *Marquis Who's Who in America* 2005.